**Article:**

Jonas, L, Mueller, T, Dohmen, R et al. (2 more authors) (2015) Transport-controlled hydrothermal replacement of calcite by Mg-carbonates. Geology, 43 (9). pp. 779-782. ISSN 0091-7613

https://doi.org/10.1130/G36934.1

# Transport-controlled hydrothermal replacement of calcite by Mg carbonates

**Laura Jonas[1*], Thomas Müller[1, *2], Ralf Dohmen[1*], Lukas Baumgartner[3*], and Benita Putlitz[3*]**

*[1]Institut für Geologie, Mineralogie und Geophysik, Ruhr-Universität Bochum,*
*[2]School of Earth and Environmental Sciences, University of Leeds, LS2 9JT Leeds, UK*
*Universitätsstrasse 150, D-44801 Bochum, Germany*
*[3]Institute of Earth Sciences, University of Lausanne, Geopolis Building, CH-1015 Lausanne, Switzerland*

*E-mails: laura.jonas@rub.de; ralf.dohmen@rub.de; t.mueller@leeds.ac.uk; lukas.baumgartner@unil.ch; benita.putlitz@unil.ch.

## ABSTRACT

Dolomitization is one of the most important diagenetic processes but the reaction rate and timescale of dolomitization remain a topic of controversy. We conducted experiments in which the reaction of single calcite crystals with a Mg-rich fluid at 200 °C leads to the formation of a zoned reaction rim consisting of magnesite and for intermediate times Ca-rich dolomite. From detailed documentation of the evolution of the microtexture and chemical composition of the reaction rim we infer a kinetic model for calcite replacement by Mg-carbonates. The chemical gradient for the structure forming elements Mg and Ca in the reaction rim and the evolution of the rim thickness strongly indicate that the overall reaction rate is controlled by diffusive transport through the porous reaction rim. The composition of the product phases is kinetically controlled and

records the local composition of the interfacial fluid without requiring oversaturation of the reservoir fluid. Reactive transport models on dolomitization processes assume that the rate of dolomitization depends on the rate of dolomite precipitation, which is contradictory to our experimental evidence. Modeling carbonate replacement in natural systems requires detailed knowledge on the evolution of the microstructure controlling the physicochemical transport properties of elements in the pore fluid.

## INTRODUCTION

Dolomites comprise a large fraction of oil and gas reservoir rocks and are of substantial economic importance. The formation of dolomite is commonly considered to take place by the replacement of a precursor limestone. Reactive transport models are used to predict the rates and spatial patterns of dolomitization (e.g., Wilson et al., 2001; Jones and Xiao, 2005; Whitaker and Xiao, 2010) and apply data from dolomite precipitation experiments (e.g., Arvidson and Mackenzie, 1999) to calculate the overall reaction rate. The replacement reaction consists of a series of processes including dissolution, transport and precipitation (e.g., Mueller et al., 2010, and references therein). The use of precipitation rates is only justified if precipitation is the slowest and thus rate limiting process, which is not yet experimentally proven.

Hydrothermal carbonate-carbonate replacement experiments were carried out to investigate the stability fields in different carbonate-fluid systems with saline solutions of different composition. Most of these studies used saline solutions to react with powdered carbonate materials with high reactive surface to solid volume ratios (e.g., Graf and Goldsmith, 1955; Katz and Matthews, 1977; Kaczmarek and Sibley, 2011).

Hydrothermal experiments on replacement of fragments of recent and fossil biogenic carbonates by dolomite (e.g., Bullen and Sibley, 1984; Grover and Kubanek, 1983) and single aragonite crystals by calcite (e.g., Perdikouri et al., 2011) were conducted. Since many studies on carbonate replacement are based on experiments with powdered material, no detailed studies of the developing microstructures accompanying the replacement of single calcite crystals by Mg carbonates have been published to date. We present a series of hydrothermal experiments using single calcite crystals and Mg-rich fluid to gain understanding of the mechanisms and rates controlling the replacement. The use of single crystals with planar surfaces and homogeneous composition allows to study the evolving microstructures and to analyze the reaction product's chemical composition with high spatial resolution. Coupling information on the microstructures with chemical data and reaction rates enables a quantitative description of the element fluxes controlling the reaction progress. Our results demonstrate that element transport on the grain scale, rather than the precipitation rate, is controlling the local fluid chemistry, the precipitating phase and the transformation rate of an individual crystal. Identification of the rate-limiting step is crucial to develop a parameterization for the rate of dolomitization and its prediction in natural systems, e.g., for burial dolomitization in diagenetic environments.

## EXPERIMENTAL AND ANALYTICAL METHODS

Single calcite crystals (~2 × 2 × 2 mm) were split using a razorblade and reacted with a 1 M $MgCl_2$ solution prepared from anhydrous $MgCl_2$ (Sigma-Aldrich Chemie GmbH, ≥98%) and distilled water. In each experiment, one crystal and 1 mL of liquid were placed into a Teflon$^{©}$-lined steel autoclave and reacted at 200 °C at vapor-saturated conditions (~16 bars). Five experiments were performed with times of 1, 3, 7, 14, and 28 days. After reaction, the autoclaves were removed from the furnace and cooled to room temperature in ~60 min. The fluid was removed from the reactors and analyzed using atomic absorption spectroscopy (AAS). The crystals were washed with distilled water and dried at ~120 °C for 30 min. Internal features were imaged using non-destructive computed X-Ray micro-tomography (μCT). The microstructures on the surface and within cross sections of reacted crystals were analyzed using scanning electron microscopy (SEM). The chemical composition was measured using electron microprobe analysis (EMPA). Details on all analytical methods used can be found in the GSA Data Repository[1].

## RESULTS

Mineral-fluid interaction causes the replacement of calcite by a Mg-carbonate phase, either magnesite and/or a Ca-Mg-carbonate with dolomitic composition (Fig. 1). The overall reaction is characterized by the formation of a porous, sometimes layered reaction rim that progresses continuously toward the center of the crystal. A remarkable microstructural characteristic is the formation of a gap separating the rim from the unreacted core, which is also visible in 3-D μCT images (Fig. 1B). The width of both the rim and the gap increases with time. The rim evolves through three stages (see Fig. DR2 in the Data Repository). In the first stage, i.e., after 1–3 days, a thin magnesite layer replaces the outermost parts of the crystal. In experiments with intermediate run durations (~14 days), Ca-rich dolomite appears as a second product forming an intermediate layer between the calcite core and the magnesite rim. In the final stage (>28 days), only a thin layer of dolomite remains, and the rim consists almost solely of magnesite. Both the overall size and shape of the parent crystal are preserved during the replacement. The polycrystalline reaction rim is built of small Mg-carbonate rhombs (see Fig. DR3). The whole reaction rim exhibits a non-homogeneously distributed porosity with a coarse porosity in the magnesite layer and a fine porosity in the dolomite layer. When magnesite replaces dolomite in later stages of the reaction, the newly formed magnesite “inherits” the fine porosity of the dolomite precursor.

The reaction rim has a complex geometry. µCT analysis show that the thickness of individual layers depends on the orientation and position of the respective cross section. Cross sections of the crystals prepared for SEM and EMPA reveal that the total fraction $\zeta$, i.e., the fraction of calcite transformed to Mg-carbonate, increases linearly with the square root of time.

The composition of the individual layers is not homogeneous. With increasing distance from the unreacted core the Mg concentrations increase while the amount of Ca decreases. These gradients are particularly pronounced in the magnesite layer (see Fig. DR1).

Continuous Mg-Ca exchange between mineral and fluid is also recorded by the time-dependent change in fluid composition. The bulk fluid is progressively enriched in Ca and depleted in Mg. The Ca/Mg ratio of the solution increases linearly with the square root of time (Fig. 2C).

## DISCUSSION

### Microstructures and Reaction Mechanisms

The exchange reaction between crystal and fluid involves the release of elements from the dissolving parent phase into the fluid and incorporation of elements from the fluid into the product phase:

$$CaCO_3\ (s) + x\ Mg^{2+}\ (aq) \rightarrow Ca_{1-x}Mg_xCO_3\ (s) + x\ Ca^{2+}\ (aq). \qquad (1)$$

The equation describes the dissolution of the solid (*s*) calcite that immediately reacts at the interface with an aqueous (*aq*) $Mg^{2+}$ ion to precipitate Mg-carbonate. Simultaneously, a $Ca^{2+}$ ion is released into the fluid. With increasing reaction progress, the fluid reservoir becomes enriched in Ca and depleted in Mg. Continuous reaction progress requires effective flux of Mg from the fluid reservoir through the reaction rim toward the reaction interface, countered by a flux of Ca in the opposite direction. The transport distance continuously increases with the growth of the rim (Fig. 3A). Both the observed sharp boundaries between the product layers and the core as well as the formation of small rhombs building the rim are characteristic of a dissolution-precipitation mechanism (see review of Putnis, 2009). The pseudomorphic replacement is accompanied by a maximum negative molar volume change ($\Delta V$) of ~13% in the case of calcite being replaced by stoichiometric dolomite and ~23% for replacement by pure magnesite. The formation of interconnected porosity enables the reaction to progress further into the crystal (Putnis et al., 2005; Raufaste et al., 2011) and maintains the continuous element exchange between the fluid at the reaction interface and the fluid reservoir surrounding the crystal. However, the presence and size of the gap separating the rim from the unreacted calcite suggest that the gap comprises most of the volume loss. Some authors argue that the relative solubility of the phases contributes to the formation of porosity and the gap at the interface (e.g., Putnis, 2009). However, our calculations show that only a minor amount of calcite needs to be dissolved to saturate the bulk fluid with magnesite and hence the gap is the result of the serial nature of the reaction in combination with the large negative molar volume change.

## Kinetic Model

The overall replacement comprises a serial process of dissolution, transport and precipitation, all of which proceed at different rates (e.g., Mueller et al. 2010). The net conversion rate is controlled by the slowest, rate-limiting step in this series of sub-processes. The rate of replacement and its controlling parameters can be inferred by the time-dependent data such as the thickness of the rim and the evolution of the pore fluid chemistry, which both approximately follow a parabolic rate law characteristic for a diffusion-controlled process (Fig. 2). Rim thickness varies significantly within each sample, which can be explained by local variation of the different fluxes due to limited accessibility to the fluid or the surfaces at the bottom of the crystal sitting on the capsule wall or 3-D effects for the diffusive flux at the crystal edges. The chemical gradient within each layer mirrors the flux of Mg toward the reaction interface, countered by the flux of Ca (Fig. 3A). The gradient in the solid reaction product is a proxy for the evolution of the fluid composition at the reaction interface as the reaction rim grows under local oversaturation with regard to the respective product phase.

In the first stages of the reaction, the Ca/Mg ratio in the fluid is still low and the removal of $Ca^{2+}$ from the reaction interface is efficient enough to produce almost pure magnesite (Fig. 3B, stage 1). The width of the rim, i.e., the transport distance between the fluid reservoir and the fluid at the reaction interface, continuously increases and the removal of $Ca^{2+}$ from the interface and the supply of $Mg^{2+}$ from the reservoir toward the interface become less efficient. Consequently, the Ca/Mg ratio in solution increases with increasing distance from the fluid reservoir. This leads to an increased incorporation of $Ca^{2+}$ into the magnesite that replaces calcite, i.e., the presence of a concentration gradient within the fluid causes the distinct compositional gradient within the product layer. At some point, the increasing Ca/Mg ratio in the interfacial fluid leads to supersaturation with respect to dolomite and facilitates dolomite nucleation. Thus a dolomite layer develops between the magnesite layer and the calcite (Fig. 3B, stage 2). In later stages of the replacement, the system approaches chemical equilibrium. Dissolution of calcite decelerates, whereas the concentration of Mg in the reservoir fluid is still high enough to supply the pore fluid with Mg. The fluid at the magnesite-dolomite interface becomes supersaturated with respect to Ca-bearing magnesite. This leads to the secondary replacement of dolomite by magnesite (Fig. 3B, stage 3):

$$Ca_xMg_{1-x}CO_3\ (s) + y\ Mg^{2+}\ (aq) \rightarrow Ca_{x-y}Mg_{(1-x)+y}CO_3\ (s) + y\ Ca^{2+}\ (aq). \qquad (2)$$

At the final stage, the growth of magnesite is faster compared to dolomite, which must be related to a more efficient element transport within the magnesite layer. Enhanced porosity in the newly formed magnesite related to the volume change of Reaction 2 could be the reason since no gap formed at the magnesite-dolomite interface.

Therefore, we can explain our observations consistently assuming that the reaction is controlled by diffusion through the pore fluid. If one of the other serial processes (dissolution or precipitation) would be rate-limiting, the reaction could be classified as interface-controlled, but this would imply a homogeneous fluid composition throughout the reaction system (Lasaga, 1986). It is impossible to explain the appearance and disappearance of dolomite assuming a homogeneous but evolving fluid composition since the observed Ca/Mg ratio in the fluid reservoir continuously increases and cannot explain sudden under-saturation with respect to dolomite in the later stage. When dolomite becomes undersaturated, the fluid at the magnesite-dolomite interface must have had a different composition compared to the fluid reservoir indicating gradients in the pore fluid.

We note, however, that most natural fluids contain higher Ca/Mg ratios than the reservoir fluid of our experiments. Thus, for natural dolomitization processes the formation of magnesite is likely omitted.

## IMPLICATIONS FOR OVERALL REACTION RATES OF DOLOMITIZATION

Pseudomorphic replacement has been reported for other carbonate-carbonate replacements taking place by dissolution-precipitation (e.g., Grover and Kubanek, 1983; Bullen and Sibley, 1984; Perdikouri et al., 2011) and appears to be the most likely mechanism for dolomitization. Our experimental study illustrates the influence of fluid composition, i.e., the cation ratio in the reacting fluid, on the precipitating phase(either magnesite or dolomite) and its composition in agreement with previous studies (e.g., Rosenberg et al., 1967; Sibley, 1990; Tribble et al., 1995; Kaczmarek and Sibley, 2011). However, to predict rates of dolomitization (or other carbonate replacements) an appropriate kinetic law needs to be formulated. Previous studies concluded that the rate of hydrothermal dolomitization increases with temperature, surface area, fluid-rock ratio, the concentration and Mg/Ca ratio of the solution (e.g., Katz and Matthews, 1977; Sibley et al., 1987; 1994; Sibley, 1990), all of which are consistent with a reaction that is controlled by diffusion through the fluid network. Here, an increase in surface area, temperature and Mg concentration in solution results in an increase of the net diffusion flux of Mg towards the unreacted calcite crystal and thus the overall reaction rate. Some experimental studies using powdered material applied an empirical Avrami-type transformation equation to interpret their rate data, since the reaction progress revealed the typical S-shaped pattern of Avrami-type transformation curves (Sibley, et al., 1987; Sibley, 1990). The exponential growth law approximated in Avrami's equation applies for linear growth and is approximately valid for early stages of diffusion-controlled growth (Christian, 1975). Diffusion controlled growth as defined by Christian (1975) refers to the growth of an isolated precipitate particle in a homogeneous medium of another phase. This is not the case in our experiments and earlier powder experiments. Thus, the quantitative extrapolation of reaction rates based on powder experiments to natural systems using an empirical Avrami equation may yield misleading interpretations with regard to the reaction rate of the overall replacement process.

Despite the existence of Avrami-type rate data for carbonate replacement, reactive transport models on hydrothermal dolomitization in natural systems are often based on the assumption that the rate of Mg-carbonate precipitation is the rate-limiting step controlling the replacement of individual crystals. In this case, the formation rate of dolomite is controlled by three parameters: temperature, surface area and saturation index (Arvidson and Mackenzie, 1999). The surface area is coupled to the grain size whereas the saturation index is related to diffusive, dispersive and advective transport of aqueous species through the fluid network. From our experiments we infer a different quantitative effect of the texture on the reaction progress and overall rate. The dolomitization rate at a specific site is strongly grain-size dependent due to different transport distances through the newly formed polycrystalline rim but also related to 3-D effects of the diffusive flux (note the pronounced reaction rate at the crystal edges visible in the µCT images, see appendix). The overall rate of dolomitization is then controlled by the supply through the larger fluid network and the transport through the rim. The spread of the reaction front and the related reaction rates would differ significantly from the case of a precipitation rate controlled reaction. Our observations strongly indicate that, for calcite replacement, the diffusive transport within the pore fluid of the evolving reaction rim is the rate-limiting step. Our observations and kinetic model provide a better basis to develop a new parameterization of dolomitization rates that could be used for macroscopic models and to constrain the temporal and spatial extent of burial dolomitization through highly saline waters and oilfield brines.

## ACKNOWLEDGMENTS

This study was financially supported by German Research Foundation grant MU2988/2-1 to Müller and Dohmen. Stimulating discussions with John Ferry, Adrian Immenhauser, Sumit Chakraborty, Andrew Putnis, and Vanessa Helpa are greatly acknowledged. We thank Shaun Barker and four anonymous reviewers for their constructive comments, and editor J. Brendan Murphy for the handling of this manuscript and additional helpful comments.

## REFERENCES CITED

Arvidson, R.S., and Mackenzie, F.T., 1999, The dolomite problem: Control of precipitation kinetics by temperature and saturation state: American Journal of Science, v. 299, p. 257–288, doi:10.2475/ajs.299.4.257.

Bullen, S.B., and Sibley, D.F., 1984, Dolomite selectivity and mimic replacement: Geology, v. 12, p. 655–658, doi:10.1130/0091-7613(1984)12<655:DSAMR>2.0.CO;2.

Christian, J.W., 1975, The theory of transformations in metals and alloys: New York, Pergamon Press, 1200 p.

Graf, D.L., and Goldsmith, J.R., 1955, Dolomite-magnesian calcite relations at elevated temperatures and $CO_2$ pressures: Geochimica et Cosmochimica Acta, v. 7, p. 109–128, doi:10.1016/0016-7037(55)90023-5.

Grover, J., and Kubanek, F., 1983, The formation of ordered dolomite from high-magnesium calcite at 250 °C to 350 °C and 1500 bars: Epitactic growth with optimal phase orientation, and implications for carbonate diagenesis: American Journal of Science, v. 283-A, p. 514–539.

Jones, G.D., and Xiao, Y., 2005, Dolomitization, anhydrite cementation, and porosity evolution in a reflux system: Insights from reactive transport models: AAPG Bulletin, v. 89, p. 577–601, doi:10.1306/12010404078.

Kaczmarek, S.E., and Sibley, D.F., 2011, On the evolution of dolomite stoichiometry and cation order during high temperature synthesis experiments: An alternative model for the geochemical evolution of natural dolomites: Sedimentary Geology, v. 240, p. 30–40, doi:10.1016/j.sedgeo.2011.07.003.

Katz, A., and Matthews, A., 1977, The dolomitization of $CaCO_3$: An experimental study at 252 - 295 °C: Geochimica et Cosmochimica Acta, v. 41, p. 297–308, doi:10.1016/0016-7037(77)90238-1.

Lasaga, A.C., 1986, Metamorphic reaction rate laws and development of isograds: Mineralogical Magazine, v. 50, p. 359–373, doi:10.1180/minmag.1986.050.357.02.

Mueller, T., Watson, E.B., and Harrison, T.M., 2010, Applications of Diffusion Data to High-Temperature Earth Systems, *in* Zhang, Y., and Cherniak, D., eds., Diffusion in Minerals and Melts: Reviews in Mineralogy and Geochemistry 72, p. 997–1038.

Perdikouri, C., Kasioptas, A., Geisler, T., Schmidt, B.C., and Putnis, A., 2011, Experimental study of the aragonite to calcite transition in aqueous solution: Geochimica et Cosmochimica Acta, v. 75, p. 6211–6224, doi:10.1016/j.gca.2011.07.045.

Putnis, A., 2009, Mineral Replacement Reactions: Reviews in Mineralogy and Geochemistry, v. 70, p. 87–124, doi:10.2138/rmg.2009.70.3.

Putnis, C.V., Tsukamoto, K., and Nashimura, Y., 2005, Direct observation for pseudomorphism: Compositional and textural evolution at a solid-fluid interface: The American Mineralogist, v. 90, p. 1909–1912, doi:10.2138/am.2005.1990.

Raufaste, C., Jamtveit, B., John, T., Meakin, P., and Dysthe, D.K., 2011, The mechanism of porosity formation during solvent-mediated phase transformations: Proceedings - Royal Society. Mathematical, Physical and Engineering Sciences, v. 467, p. 87–124.

Rosenberg, P.E., Burt, D.M., and Holland, H.D., 1967, Calcite-dolomite-magnesite stability relations in solutions: The effect of ionic strength: Geochimica et Cosmochimica Acta, v. 31, p. 391–396, doi:10.1016/0016-7037(67)90049-X.

Sibley, D.F., 1990, Unstable to stable transformations during dolomitization: The Journal of Geology, v. 98, p. 739–748, doi:10.1086/629437.

Sibley, D.F., Dedoes, R.E., and Bartlett, T.R., 1987, Kinetics of dolomitization: Geology, v. 15, p. 1112–1114, doi:10.1130/0091-7613(1987)15<1112:KOD>2.0.CO;2.

Sibley, D.F., Nordeng, S.H., and Borkowski, M.L., 1994, Dolomitization kinetics in hydrothermal bombs and natural settings: Journal of Sedimentary Research, v. 64, p. 630–637, doi:10.1306/D4267E29-2B26-11D7-8648000102C1865D.

Tribble, J.S., Arvidson, R.S., Lane, M., III, and Mackenzie, F.T., 1995, Crystal chemistry, and thermodynamic and kinetic properties of calcite, dolomite, apatite, and biogenic silica: Applications to petrologic problems: Sedimentary Geology, v. 95, p. 11–37, doi:10.1016/0037-0738(94)00094-B.

Whitaker, F.F., and Xiao, Y., 2010, Reactive transport modeling of early burial dolomitization of carbonate platforms by geothermal convection: AAPG Bulletin, v. 94, p. 889–917, doi:10.1306/12090909075.

Wilson, A.M., Sanford, W., Whitaker, F., and Smart, P., 2001, Spatial patterns of diagenesis during geothermal circulation in carbonate platforms: American Journal of Science, v. 301, p. 727–752, doi:10.2475/ajs.301.8.727.

## FIGURE CAPTIONS

Figure 1. Backscattered electron image of a polished cross section of a crystal that reacted for 2 weeks (A) shows that the rim is divided into two layers consisting of magnesite and dolomite. µCT analysis of a crystal with the same reaction time (B) allows a three-dimensional reconstruction of the sample. The different layers of the reaction rim and the unreacted core can be distinguished due to the different X-ray attenuation and densities of the respective mineral phases. µCT cross sections show that a gap located at the reaction interface separates the reaction rim from the calcite core.

Figure 2. A: Fraction of unreacted calcite and fraction transformed to magnesite and dolomite as a function of time. Both the fraction of unreacted calcite and the total fraction transformed as a function of time follow an exponential trend ($R^2 = 0.98$). The total fraction transformed $\zeta$ (B) and the Ca/Mg ratio of the reacted fluid (C) can be fitted with a square root of time relation.

Figure 3. A: The growth of the reaction front depends on the flux of the relevant aqueous species ($J_{Mg^{2+}}$, $J_{Ca^{2+}}$, $J_{CO_3^{2-}}$) in the fluid and is accompanied by a considerable molar volume change ($\Delta V$). B: The fluid composition in the rim changes with time. In early stages of the reaction, the ion activity product (IAP) of magnesite in the interfacial fluid exceeds the equilibrium solubility product (K) of magnesite, i.e., the saturation index $[SI = -\log(\frac{IAP}{K})]$ with respect to magnesite at the interface is >0 and magnesite precipitates (stage 1). After 7 days, the Ca-concentration at the interface increases and the SI of dolomite is reached (stage 2). In the final stages, the Mg-concentration at the interface increases, and the fluid becomes supersaturated with respect to magnesite (stage 3).

[1] GSA Data Repository item 2015xxx, xxxxxxxx, is available online at www.geosociety.org/pubs/ft2015.htm, or on request from editing@geosociety.org or Documents Secretary, GSA, P.O. Box 9140, Boulder, CO 80301, USA.

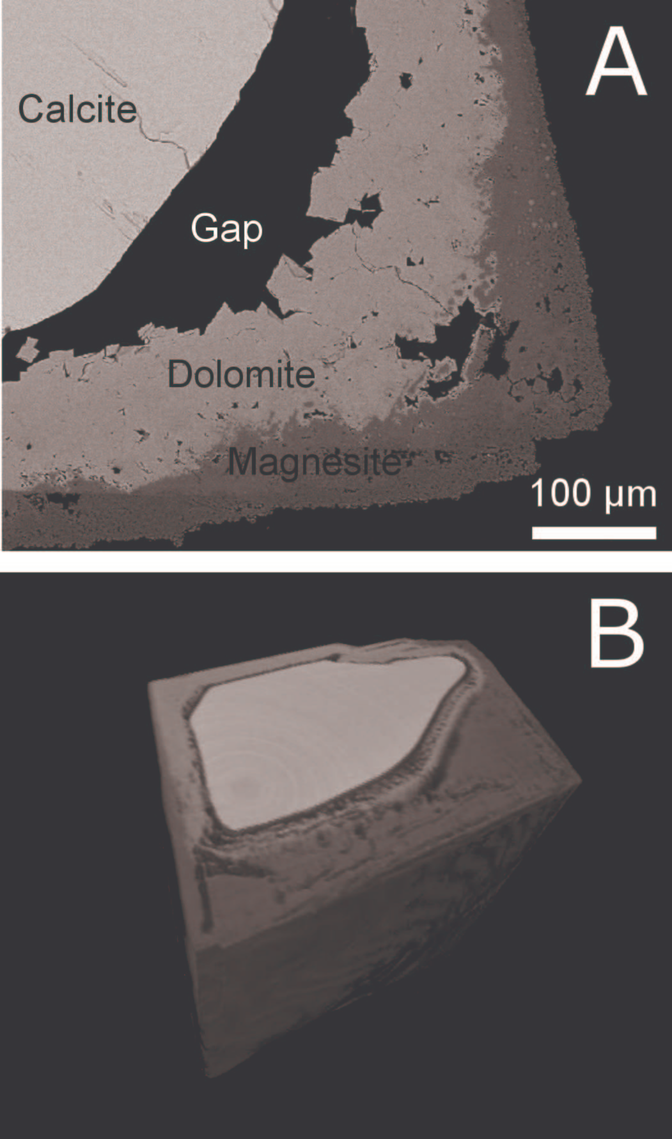
A
Calcite
Gap
Dolomite
Magnesite
100 µm
B

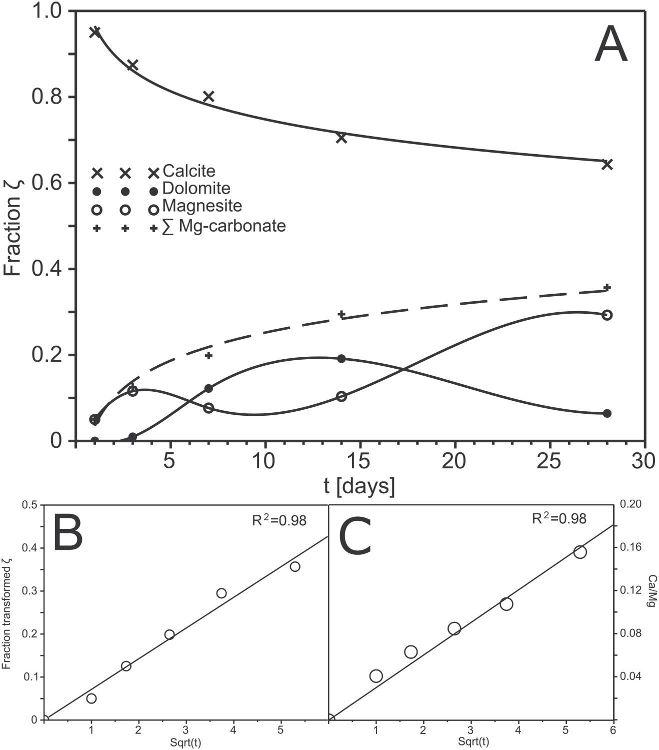
A
Calcite
Dolomite
Magnesite
∑ Mg-carbonate
Fraction ζ
1.0
0.8
0.6
0.4
0.2
0
5
10
15
20
25
30
t [days]
B
R²=0.98
Fraction transformed ζ
0.5
0.4
0.3
0.2
0.1
0
1
2
3
4
5
Sqrt(t)
C
R²=0.98
Ca/Mg
0.20
0.16
0.12
0.08
0.04
1
2
3
4
5
6
Sqrt(t)

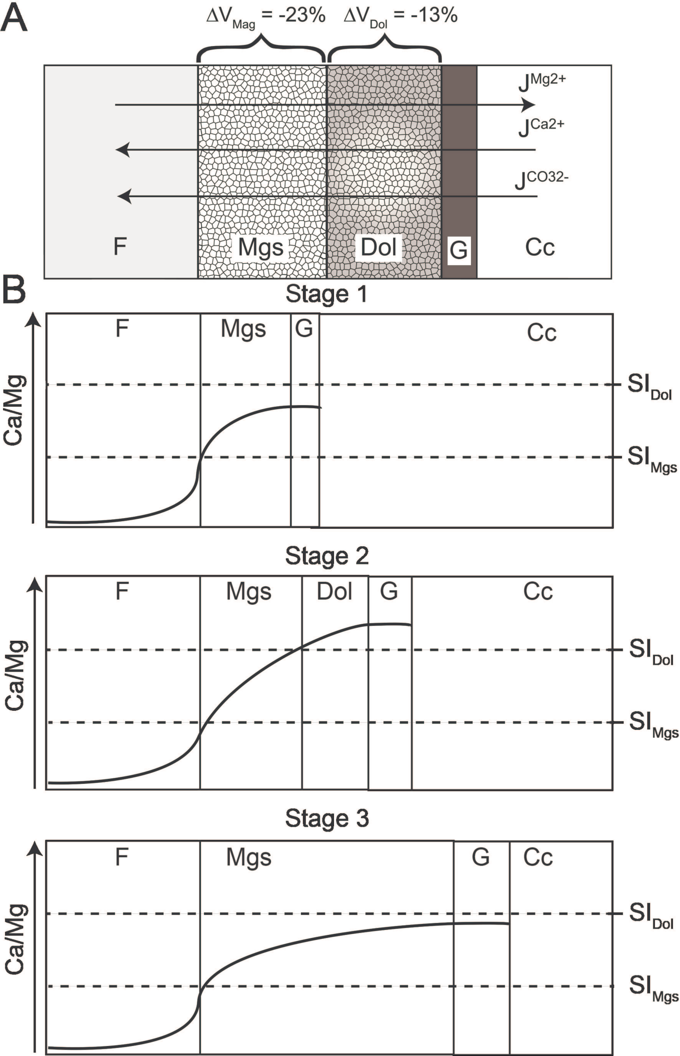
A
ΔV_Mag = -23%
ΔV_Dol = -13%
J^Mg2+
J^Ca2+
J^CO32-
F
Mgs
Dol
G
Cc
B
Stage 1
F
Mgs
G
Cc
Ca/Mg
SI_Dol
SI_Mgs
Stage 2
F
Mgs
Dol
G
Cc
Ca/Mg
SI_Dol
SI_Mgs
Stage 3
F
Mgs
G
Cc
Ca/Mg
SI_Dol
SI_Mgs